

Extreme ultraviolet holographic lithography: Initial results

Cite as: Appl. Phys. Lett. **90**, 023116 (2007); <https://doi.org/10.1063/1.2430774>

Submitted: 09 August 2006 • Accepted: 07 December 2006 • Published Online: 12 January 2007

Yang-Chun Cheng, Artak Isoyan, John Wallace, et al.



ARTICLES YOU MAY BE INTERESTED IN


Three-dimensional photonic crystals fabricated by visible light holographic lithography
Applied Physics Letters **82**, 2212 (2003); <https://doi.org/10.1063/1.1565682>

Progress in extreme ultraviolet interferometric and holographic lithography
Journal of Vacuum Science & Technology B: Microelectronics and Nanometer Structures Processing, Measurement, and Phenomena **25**, 2145 (2007); <https://doi.org/10.1116/1.2794069>





Multiple-exposure holographic lithography with phase shift
Applied Physics Letters **85**, 4184 (2004); <https://doi.org/10.1063/1.1813644>



HIDEN
ANALYTICAL



Instruments for Advanced Science

<ul style="list-style-type: none"> ■ Knowledge, ■ Experience, ■ Expertise <div style="background-color: #000080; color: white; text-align: center; padding: 5px; margin-top: 10px;"> Click to view our product catalogue </div> <p style="font-size: small; margin-top: 10px;">Contact Hiden Analytical for further details: www.HidenAnalytical.com info@hideninc.com </p>	<div style="text-align: center; margin-bottom: 10px;">  <p>Gas Analysis</p> </div> <ul style="list-style-type: none"> ▶ dynamic measurement of reaction gas streams ▶ catalysis and thermal analysis ▶ molecular beam studies ▶ dissolved species probes ▶ fermentation, environmental and ecological studies 	<div style="text-align: center; margin-bottom: 10px;">  <p>Surface Science</p> </div> <ul style="list-style-type: none"> ▶ UHVTPD ▶ SIMS ▶ end point detection in ion beam etch ▶ elemental imaging - surface mapping 	<div style="text-align: center; margin-bottom: 10px;">  <p>Plasma Diagnostics</p> </div> <ul style="list-style-type: none"> ▶ plasma source characterization ▶ etch and deposition process reaction kinetic studies ▶ analysis of neutral and radical species 	<div style="text-align: center; margin-bottom: 10px;">  <p>Vacuum Analysis</p> </div> <ul style="list-style-type: none"> ▶ partial pressure measurement and control of process gases ▶ reactive sputter process control ▶ vacuum diagnostics ▶ vacuum coating process monitoring
--	--	--	--	--

Extreme ultraviolet holographic lithography: Initial results

Yang-Chun Cheng^{a)}

Materials Science Program, University of Wisconsin-Madison, Wisconsin

Artak Isoyan and John Wallace

Center for Nanotechnology, University of Wisconsin-Madison, Wisconsin

Mumit Khan

BRAC University, Bangladesh

Franco Cerrina^{a),b)}

Department of Electrical and Computer Engineering, University of Wisconsin-Madison, Wisconsin

(Received 9 August 2006; accepted 7 December 2006; published online 12 January 2007)

The authors report the initial results from a holographic lithography technique using extreme ultraviolet (EUV) radiation. This approach removes the need for complex EUV reflective masks and optics, replacing them with a binary, nanopatterned transmission mask. Computer generated holograms were fabricated on 100 nm thick silicon nitride membranes with a 100 nm thick chromium absorber layer. Reconstructed images have been recorded in an 80 nm thick polymethylmetacrylate photoresist using 13 nm wavelength EUV radiation from an undulator source. The pattern was characterized by optical and atomic force microscopies, and compared with simulation results from the TOOLSET diffraction simulation program, yielding excellent agreement. © 2007 American Institute of Physics. [DOI: 10.1063/1.2430774]

Extreme ultraviolet lithography (EUVL) is being developed to support the fabrication of sub-32 nm electronic devices. It is based on the use of radiation around 13 nm, a region where all materials are highly absorptive and only multilayer coated reflective optics (and masks) can be used to form images of the patterns to be printed. Today, only a few exposure tools are in existence due to the combined requirements of source, complex reflective mask, and reflective imaging optics.¹ Undulator insertion devices on a synchrotron are ideal EUV sources: they have high brightness, are tunable, and exhibit good spectral and temporal coherences.² Undulator sources have indeed been used to characterize EUV optics,³ and wave front studies based on holographic techniques have been implemented.⁴ In this letter, we report on the development of EUV holograms specifically designed for patterning.

Interference lithography (IL) is widely used to form one- and two-dimensional regular patterns, mostly using laser line sources in the UV (340 nm) or deep-UV regions (248 and 193 nm).⁵ Recently, this technique has been extended to the EUV at 13 nm yielding unprecedented resolution.⁶ While EUV-IL is very useful for generating periodic patterns that can be used to characterize photoresist materials⁷ as well as creating templates for guided self-assembled geometries,⁸ it is limited by its very nature to periodic structures. A natural extension of EUV-IL can be EUV *holographic* lithography (EUV-HL), where a computer generated hologram (CGH) patterned on a suitable carrier is used to project an image on a given substrate. This approach has the great advantage of not relying on complex optical systems to form the image.

The experimental setup of a transmissive EUV-HL system is shown in Fig. 1: it requires of course a hologram, a source, and a recording medium. The CGH can be fabricated

as a transmission or reflection object, as discussed below. Being a diffractive optic, the resolution of the image formed is limited mainly by the patterning pixel while the size of the exposed area is determined by the spatial coherence of the source. Using modern nanofabrication techniques, it is possible to pattern CGHs with sub-30 nm resolution as demonstrated by the commercially available high-resolution Fresnel zone plates (FZPs) currently in use at many photon sources.⁹

It is well known that a hologram is generated by recording the interference of a coherent reference wave front with the wave fronts diffracted or scattered by an object. In reverse, when a coherent wave front interferes with the hologram, the reconstruction of the object is formed at the imaging plane of the hologram, i.e., where the real object was originally located. The goal of HL is to expose a given target pattern from a *synthetic hologram*, a CGH, since no object is

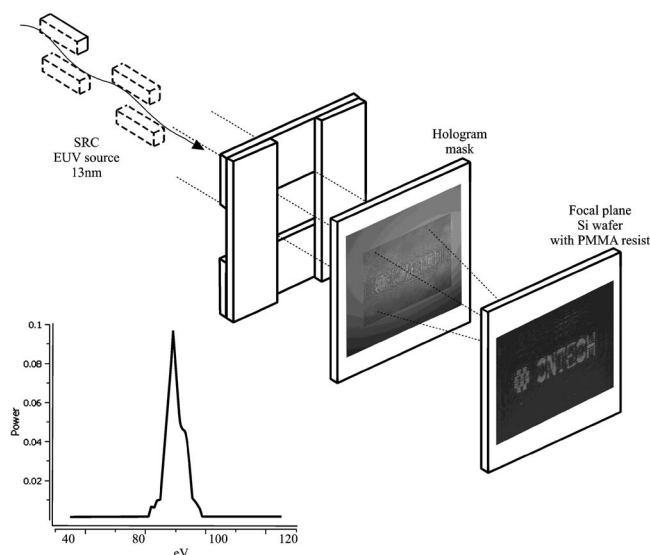


FIG. 1. Experimental setup used for EUV-HL.

^{a)}Also at Center for Nanotechnology, University of Wisconsin-Madison.

^{b)}Electronic mail: fcerrina@wisc.edu

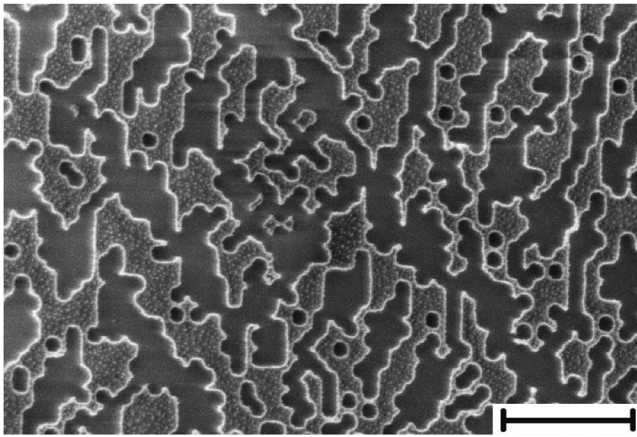


FIG. 2. SEM image of the Cr binary computer generated hologram after dry etching. The scale bar indicates 1 μm .

available to record the hologram itself. While HL has been proposed and implemented in commercial lithographic tools,¹⁰ for the near UV, the rapid development of optical steppers has quickly taken over the field of UV lithography. The situation is entirely different in the EUV, because there are only very few imaging systems that have been developed.¹ EUV-HL provides an effective pathway for the development of EUV lithography: while it is a $1\times$ system because the resolution is limited by the patterning pixel size, its main advantage is that CGHs do not require complex optical systems to image a mask—the mask itself is the optical system. In addition, the binary nature of the mask, in principle, makes it possible to design a CGH that works in the third order, thus yielding a $3\times$ demagnification of the pattern projected. We note that the information required for image formation is spread out over the entire hologram, so that the image quality is less sensitive to mask defects.

As a demonstration of EUV-HL, we decided to print the logo of the Center for Nanotechnology (CNTECH) using the undulator source at the Synchrotron Radiation Center. The design of the CGH is relatively simple. Given the wavelength, layout, and focal distance we compute the diffraction pattern of the layout, form the interference with the reference beam, and thus define the hologram itself. We note that this is an in-line hologram, i.e., a Gabor hologram.¹¹ In the EUV spectral region, a transmissive object must be based on thin membranes. We use 100 nm of SiNH (silicon-rich nitride) as the carrier, with a transmission $T \approx 10\%$. A thin 100 nm Cr film (absorption coefficient $\mu = 0.28 \mu\text{m}^{-1}$ at 13 nm) is sufficient to absorb completely the radiation, with a transmission $T \approx 3\%$. Thus, our CGH is realized in a thin Cr absorber patterned on a thin membrane. Because of the planar fabrication procedure, the CGH must be a binary rather than a continuous tone object. The “CNTECH” word was introduced as a binary mask in our TOOLSET diffraction simulation program.¹² The electric field diffracted from a coherent light source with $\lambda = 13 \text{ nm}$ was recorded at the position 1500 μm away from the mask. The pixel size for the calculation was $80 \times 80 \text{ nm}^2$, and the field size was 1024×1024 pixels, i.e., approximately $80 \times 80 \mu\text{m}^2$. The CGH is calculated from the equation describing the intensity distribution, i.e., $(1 + E_{\text{real}})^2 + E_{\text{imag}}^2$,¹¹ where the reference beam is normalized to 1, and converted to a binary mask pattern by thresholding the image using a nonlinear algorithm. As a test, we also computed (and fabricated) an identical but larger

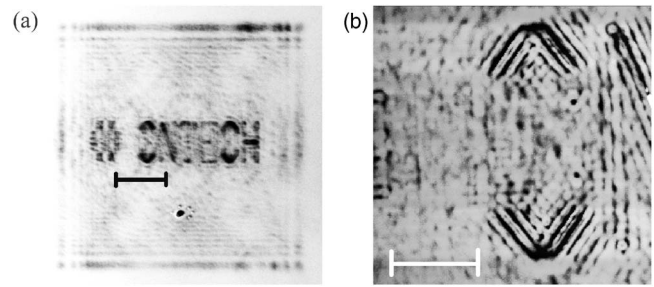


FIG. 3. Reconstructed holographic image recorded on PMMA resist. An optical microscopy image is shown in (a) with a black scale bar indicating 15 μm . An AFM image of the letter “C” above the black scale bar in (a) is shown in (b) with a white scale bar indicating 5 μm .

CGH pattern scaled to yield an image with $800 \times 800 \text{ nm}^2$ pixel size ($800 \times 800 \mu\text{m}^2$ field size), and focal distance of 15 cm at EUV wavelength. We note that in order to have a point resolution of 80 nm at the EUV wavelength of 13 nm, the CGH must have a numerical aperture of at least ≈ 0.08 ; thus, for a distance of 1.5 mm the CGH should be at least 240 μm in diameter. For a finite size object, the CGH would be correspondingly larger. In our case the physical size is 80 μm , so that the resolution is less than that of the full hologram.

The actual fabrication process is based on one of the standard processes developed at CNTECH for creating x-ray diffractive optics. A low-stress 100 nm thick low-pressure chemical vapor deposited SiNH was deposited on 4 in. (100) Si wafers. A standard reactive ion etching process using CHF_3 gas chemistry was used to pattern etch windows in the back side nitride layer using SC1827 resist. A Cr absorber layer with thickness $\approx 100 \text{ nm}$ was deposited on the front surface by a Telemark CHA-600 E-beam evaporator. A JEOL JBX-5D2 e-beam lithography tool with 50 keV beam energy was used to pattern the CGH in 250 nm of UV3 resist. An etching process utilizing SF_6 and O_2 chemistry was developed for a Plasma-Therm 770 inductively coupled plasma etching tool to transfer the CGH pattern into an underlying Cr absorber layer. A scanning electron microscopy (SEM) image of the Cr binary CGH after dry etching is shown in Fig. 2. After completing the CGH pattern, the Si in the window regions was removed by back-etching the wafer with a 20 wt % KOH solution at 90 $^\circ\text{C}$; the front side was protected with a Teflon holder. Thus, we completed the Cr binary CGH mask on the SiNH membrane.

The experimental setup has been described before.⁷ For the experiment described here, a silicon wafer was coated with 80 nm of polymethylmetacrylate (PMMA) photoresist. The CGH mask was stacked onto the wafer using spacers of thickness suitable to form the 1.5 mm gap, and held in place with magnets. The radiation from the U2 undulator was reflected on the CGH mask by a flat 45 deg multilayer mirror Mo-Si; no other optically relevant elements were present in the beamline. Exposure times were of the order of 0.5–3 s. The spectral bandwidth of the undulator (after the mirror) was about 1.2 nm. The undulator beam size was around $4 \times 4 \text{ mm}^2$ at the CGH.

After exposure and development in MIBK:IPA = 1:4 for 20 s, the reconstructed patterns were inspected with optical microscopy and atomic force microscopy (AFM). The AFM scans show clearly that the image is fully developed through the resist thickness (80 nm). SEM images from Au-coated



FIG. 4. Simulation of the reconstructed holographic image. The scale bar indicates 15 μm . Notice the excellent agreement with the pattern recorded in Fig. 3.

samples have been acquired as well, but the contrast and hence the quality are poorer than in the case of optical and scanning probe microscopies. Typical patterns are shown in Fig. 3. The images acquired by the AFM as shown in Fig. 3(b) show structures on a scale length of about 80 nm; this is consistent with the patterning pixel size on the CGH mask, and is also indicative of the very high degree of coherence of the undulator beam causing ringing in the image. Like in optical lithography, a reduction in the degree of spatial coherence will produce a smoother image.

In order to explain the somewhat uneven appearance of the resist patterns, we performed a detailed simulation study of the image formation. Again, the TOOLSET was used to predict the image intensity from the binary CGH mask exposed in the conditions described above, i.e., for a CGH 80 μm in size. The results are shown in Fig. 4. We note the excellent agreement between simulation and experiment. In particular, some of the details such as the partly missing "C" are clearly predicted. We note that several factors must be taken into account to explain the image. The CGH size is smaller than the ideal one (80 μm instead of 240 μm); this results in a lower resolution than ideally possible. Second, the conversion of the continuous tone CGH to binary will affect the intensity distribution. Third, no e-beam proximity corrections were applied to the CGH pattern. By optimizing all of these effects in the binary pattern it will be possible to recover a final shape in closer agreement with the target.

A CGH can be visualized as the superposition (product) of a set of Fresnel zone plates, each corresponding to a single pixel in the object.¹¹ In the EUV, it is difficult to create a transmissive phase object because of the ratio of the real to imaginary part of the index of refraction ($n=1-\delta+j\beta$, $\delta/\beta \approx 1$), requiring very thin absorbers. Hence, it is very difficult to create true phase holograms by using multilevel binary optics as it is possible to do in the visible and in the harder x-ray region^{13–15} where optically good dielectric materials exist. Thus, optimization of the image formation will have to rely on pattern shape correction, similar to the optical proximity correction (OPC) schemes used in optical lithography. The area of exposure is limited by the spatial coherence of the light source,¹⁶ and can be as large as several millimeters for advanced synchrotron sources. For many experimental cases, a step-and-repeat technique will allow to cover large areas. Since the CGH is a diffractive optic, the temporal coherence will affect both the resolution and the depth of

focus of the image. This can be easily evaluated by resorting to the case of a zone plate—the elemental hologram. A FZP of 50 nm resolution, focal length 1.5 mm at $\lambda=13$ nm will require an outermost zone width smaller than 41 nm to deliver a resolution better than 50 nm, over a depth of focus of ± 260 nm. These requirements are fairly relaxed, as shown in our experimental results where a resolution better than ≈ 100 nm was maintained in the exposure. We note that the ultimate resolution of a CGH is $\lambda/2$ for coherent illumination, i.e., ≈ 6 nm. While this limit is probably impractical, it should be possible to reach 20 nm resolution using advanced patterning techniques.

In summary, we have demonstrated that EUV holographic lithography can be used to generate arbitrary patterns in a simple experimental system. A CGH fabricated using standard nanolithography techniques can be used to project a desired pattern on a wafer without complex optics or reflective masks; the final resolution is controlled by the patterning pixel size. A reduced image can be generated by creating a binary CGH designed to operate on the third order focus, thus allowing resolutions of 1/3 of the patterning size. As described, the technique is well suited for small fields of view and high-resolution structures. It could be conceivably extended to a larger field by using a wider support membrane and a collimator to deliver a uniform illumination, or a next-generation free electron laser. We note also that HL can be used at wavelengths other than 13 nm, depending on the available sources.

This work was supported by the Semiconductor Research Corporation under Contract No. 2005-OC-985. This work is based in part upon research conducted at the Synchrotron Radiation Center, University of Wisconsin-Madison, which is supported by the National Science Foundation under Award No. DMR-0537588. The fabrication was performed at the Wisconsin Center for Applied Microelectronics at the University of Wisconsin-Madison.

¹B. J. Lin, J. Microlithogr., Microfabr., Microsyst. **5**, 33005 (2006), and references therein.

²H. Winick and S. Doniach, *Synchrotron Radiation Research* (Plenum, New York, 1982).

³D. T. Attwood, *Soft X-rays and Extreme Ultraviolet Radiation* (Cambridge University Press, New York, 1999).

⁴S.-H. Lee, P. Naulleau, K. A. Goldberg, C.-H. Cho, S.-T. Jeong, and J. Bokor, Appl. Opt. **40**, 2655 (2001).

⁵M. L. Schattenburg, C. Chen, P. N. Everett, J. Ferrera, P. Konkola, and H. I. Smith, J. Vac. Sci. Technol. B **17**, 2692 (1999).

⁶H. H. Solak, D. He, W. Li, S. Singh-Gasson, F. Cerrina, B. H. Sohn, X. M. Yang, and P. Nealey, Appl. Phys. Lett. **75**, 2328 (1999).

⁷I. Junarsa, M. P. Stoykovich, P. F. Nealey, Y. Ma, F. Cerrina, and H. H. Solak, J. Vac. Sci. Technol. B **23**, 138 (2005).

⁸S. O. Kim, H. H. Solak, M. P. Stoykovich, N. J. Ferrier, J. J. de Pablo, and P. F. Nealey, Nature (London) **424**, 411 (2003).

⁹See, for instance, <http://xrada.com/>

¹⁰F. Clube, S. Gray, D. Struchen, J. C. Tisserand, N. Magnon, S. Malfroy, and Y. Darbellay, Opt. Eng. (Bellingham) **34**, 2724 (1995).

¹¹A. G. Michette, *Optical Systems for Soft X rays* (Plenum, New York, 1986).

¹²M. Khan and F. Cerrina, *CNTECH Toolset User Guide* (University of Wisconsin-Madison Technical Report, 1997) (unpublished).

¹³C. Jacobsen and M. R. Howells, J. Appl. Phys. **71**, 2993 (1992).

¹⁴E. Di Fabrizio, D. Cojoc, S. Cabrini, B. Kaulich, J. Susini, P. Facci, and T. Wilhein, Opt. Express **11**, 2278 (2003).

¹⁵A. A. Firsov, A. A. Svintsov, S. I. Zaitsev, A. Erko, and V. V. Aristov, Opt. Commun. **202**, 55 (2002).

¹⁶H. H. Solak, J. Phys. D **39**, R171 (2006).